

Cite this: *Chem. Sci.*, 2022, 13, 4922 All publication charges for this article have been paid for by the Royal Society of ChemistryReceived 9th March 2022  
Accepted 3rd April 2022

DOI: 10.1039/d2sc01394k

[rsc.li/chemical-science](https://rsc.li/chemical-science)

# Nickel-catalyzed skeletal transformation of tropone derivatives via C–C bond activation: catalyst-controlled access to diverse ring systems†

Takuya Kodama,<sup>ab</sup> Kanako Saito<sup>a</sup> and Mamoru Tobisu<sup>ab\*</sup>

We report herein on nickel-catalyzed carbon–carbon bond cleavage reactions of 2,4,6-cycloheptatrien-1-one (tropone) derivatives. When a Ni/N-heterocyclic carbene catalyst is used, decarbonylation proceeds with the formation of a benzene ring, while the use of bidentate ligands in conjunction with an alcohol additive results in a two-carbon ring contraction with the generation of cyclopentadiene derivatives. The latter reaction involves a nickel–ketene complex as an intermediate, which was characterized by X-ray crystallography. The choice of an appropriate ligand allows for selective synthesis of four different products via the cleavage of a seven-membered carbocyclic skeleton. Reaction mechanisms and ligand-controlled selectivity for both types of ring contraction reactions were also investigated computationally.

## Introduction

Transition metal-mediated selective cleavage of carbon–carbon (C–C) bonds has attracted the interest of researchers, since it would allow for the direct transformation of one of the most ubiquitous bonds in organic molecules.<sup>1</sup> However, both the kinetic and thermodynamic stability of C–C bonds renders their cleavage a daunting challenge. To overcome this difficulty, several strategies, including the use of angle strain,<sup>2</sup> a directing group,<sup>1,3</sup> aromatization,<sup>4</sup> and  $\beta$ -carbon elimination,<sup>5</sup> have been successfully utilized to date. In contrast to nonpolar C–C bonds, polar C–C bonds, such as those in ketones, esters and nitriles, can be cleaved more readily by transition metals, although their bond dissociation energies are comparable to those for nonpolar C–C bonds.<sup>6</sup> Regarding the metal-mediated cleavage of C(acyl)–C bonds in ketones, although most of the reported reactions continue to depend upon the use of angle strain<sup>2</sup> or a directing group,<sup>1</sup> several notable reactions that do not involve the use of such strategies have been reported. Murakami reported on a pioneering example of the metal-mediated activation of simple, unstrained ketones by developing the decarbonylation of cyclopentanones,<sup>7</sup> while Brookhart later reported on rhodium-mediated decarbonylation of diaryl ketones.<sup>8</sup> Our group

previously reported that the decarbonylation of simple, unstrained ketones can also be mediated by a nickel/N-heterocyclic carbene (NHC) complex (Fig. 1a).<sup>9</sup> Although these reactions are notable, in that neither ring strain nor a directing group is required to activate C–C bonds, it is necessary to use a stoichiometric amount of a metal complex. Catalytic C–C bond cleavage reactions of unstrained ketones have been reported to proceed when electronically activated ketones, such as diketones,<sup>10</sup> acyl cyanides,<sup>11</sup> alkynyl ketones,<sup>12</sup> or ketones bearing a directing group<sup>13</sup> are used (Fig. 1b). The catalytic C–C bond activation of simple ketones that proceed with the aid of a 2-aminopyridine cocatalyst, which serves as a temporary or removable directing group has been reported.<sup>3c,14</sup> Although these reactions demonstrate the power of transition metals for activating otherwise unreactive C–C bonds, the scope of the catalytic transformation of C–C bonds in ketones remains limited, compared with other unreactive bonds, including C–H bonds. We envisioned that 2,4,6-cycloheptatrien-1-one (tropone)<sup>15</sup> derivatives would be suitable substrates for catalytic decarbonylation because the process involves the formation of a benzene ring which would be expected to drive the otherwise difficult C–C bond cleavage reaction. It should be noted that the decarbonylation of tropone was reported to require heating at over 600 °C (ref. 16a) or photoirradiation conditions (~1% yield).<sup>16b</sup> Herein, we report on the development of a nickel/NHC complex that can catalyze the decarbonylation of tropone derivatives with the formation of a benzene ring (one-carbon ring contraction). In addition, the use of a bidentate ligand was found to allow for an unprecedented catalytic two-carbon ring contraction reaction of tropones, leading to the formation of cyclopentadiene derivatives (Fig. 1c).

<sup>a</sup>Department of Applied Chemistry, Graduate School of Engineering, Osaka University, Suita, Osaka 565-0871, Japan. E-mail: [tobisu@chem.eng.osaka-u.ac.jp](mailto:tobisu@chem.eng.osaka-u.ac.jp)

<sup>b</sup>Innovative Catalysis Science Division, Institute for Open and Transdisciplinary Research Initiatives (ICS-OTRI), Suita, Osaka 565-0871, Japan. E-mail: [tobisu@chem.eng.osaka-u.ac.jp](mailto:tobisu@chem.eng.osaka-u.ac.jp)

† Electronic supplementary information (ESI) available. CCDC 2115589–2115595. For ESI and crystallographic data in CIF or other electronic format see <https://doi.org/10.1039/d2sc01394k>



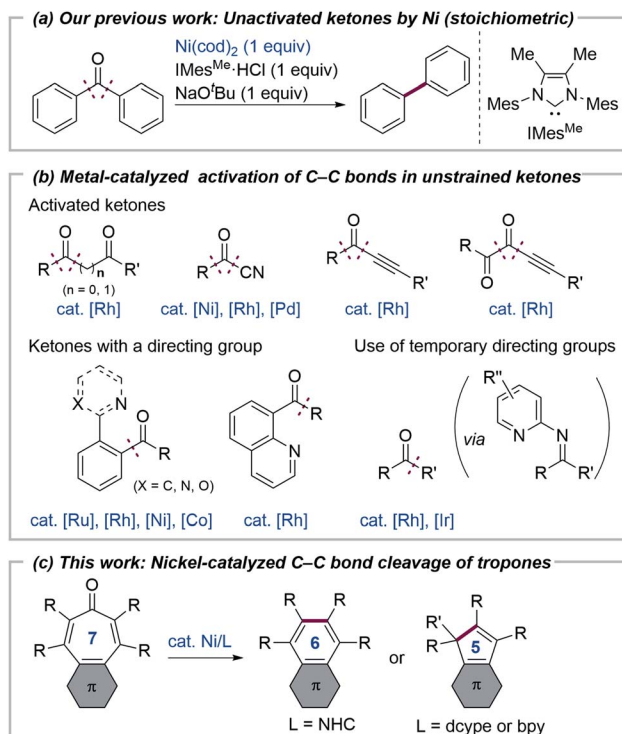


Fig. 1 Transition metal-catalyzed C–C bond activation of ketones.

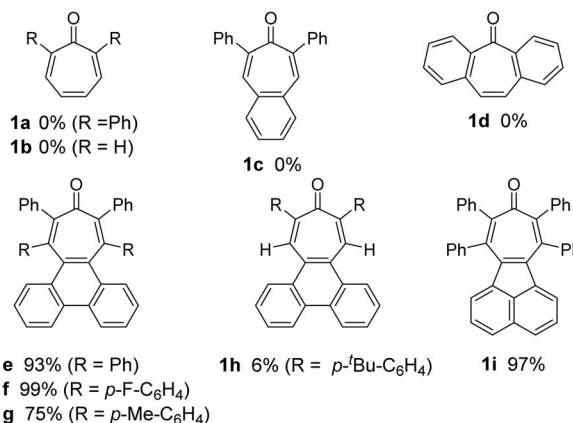
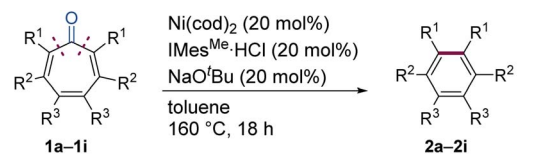


Chart 1 Scope of Ni/IMes<sup>Me</sup>-catalyzed decarbonylation of tropones. Reaction conditions: **1a** (0.20 mmol), Ni(cod)<sub>2</sub> (0.040 mmol), IMes<sup>Me</sup>.HCl (0.040 mmol), NaOtBu (0.040 mmol) toluene (1.0 mL), 160 °C for 18 h; run on a 0.30 mmol scale for **1b–1d** and on a 0.20 mmol scale for **1e–1i**.

## Results and discussion

### Catalytic decarbonylation reactions

We initiated our study by examining the decarbonylation of a series of troponone derivatives **1a–1d** using Ni(cod)<sub>2</sub> (20 mol%) and IMes<sup>Me</sup> (20 mol%), which was used as an optimal catalyst in our previously reported nickel-mediated decarbonylation of simple ketones,<sup>9a</sup> in toluene at 160 °C for 18 h (Chart 1). No reaction occurred, however, and the starting ketones were recovered quantitatively under these conditions. Interestingly, the expected decarbonylation, in fact, proceeded, when a troponone bearing a fused phenanthrene ring (*i.e.*, **1e**) was used as a substrate, providing **2e** in 93% yield. The 4,5-phenanthrene-fused tropones **1f** and **1g** bearing aryl substituents at  $\alpha$ - and  $\beta$ -positions afforded the desired decarbonylated products **2f** and **2g** in a similar manner, whereas a troponone derivative lacking  $\beta$ -substituents, *i.e.*, **1h**, gave only a 6% yield. The acenaphthylene-fused analog **1i** was decarbonylated successfully to furnish **2i** in 97% yield.

Although tropones **1a–1i** would all be expected to gain aromatic stabilization energy by decarbonylation, their reactivities toward the Ni/IMes<sup>Me</sup> catalyst were completely different. To obtain insights into structure/reactivity relationships, several structural and spectroscopic properties of the examined troponone derivatives were compared (Table 1). X-ray crystallographic analysis revealed that the C $\alpha$ –C=O bond lengths of the successfully decarbonylated substrates **1e**<sup>17a</sup> and **1i**<sup>17b</sup> were relatively longer, and the bent angles of the troponone rings ( $\theta$  and  $\varphi$  in Table 1) were larger than those for less reactive substrates **1c** and **1h**. All of these data suggest that the carbonyl groups in

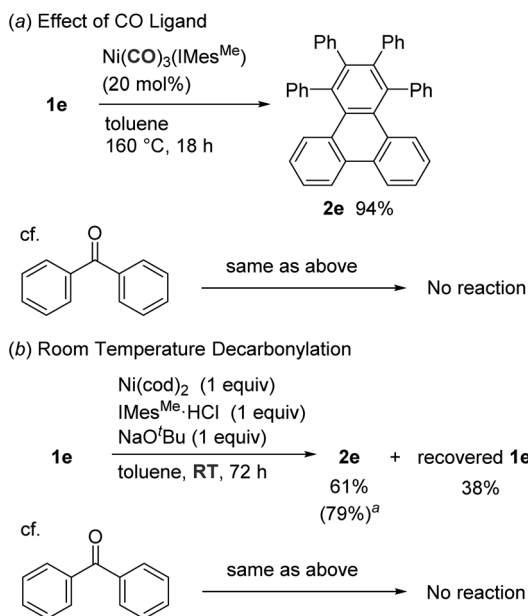
Table 1 ORTEP drawings, C–C and C–O bond lengths, and bent angles of troponone scaffolds<sup>a</sup>

	<b>1c</b>	<b>1h</b>	<b>1e</b>	<b>1i</b>
C $\alpha$ –C=O/Å	1.48	1.49	1.51	1.51
$\theta$ /deg.	~0	51.6	57.5	62.1
$\varphi$ /deg.	~0	28.4	43.2	32.8
<sup>13</sup> C-NMR (C <sub>C=O</sub> )/ppm	187	194	200	197

<sup>a</sup>  $\theta$  and  $\varphi$  are the bent angles between the meanplanes (C2–C3–C6–C7 and C1–C2–C7) and (C2–C3–C6–C7 and C3–C4–C5–C6), respectively. Structural parameters for **1e** (CCDC 2036614),<sup>17a</sup> **1h** (CCDC 2100026)<sup>17b</sup> were abstracted from the Cambridge Structural Data Base.

**1e** and **1i** are not conjugated with the  $\pi$ -system of the troponone ring in the solid state. <sup>13</sup>C-NMR chemical shifts of the carbonyl carbons of **1e** and **1i** indicated that they were more deshielded than those of **1c** and **1h**, suggesting that **1e** and **1i** also behave as the non-conjugated ketones in solution. These bent structures found in **1e** and **1i** can be attributed to van der Waals (vdW) repulsion between the  $\beta$ -substituents and a large  $\pi$ -system fused to the troponone core. These analyses suggest that ground state destabilization by vdW strain<sup>18</sup> is the key factor in





Scheme 1 Comparison between fused tropone and benzophenone.  
<sup>a</sup>Run at 40 °C for 18 h.

promoting the C–C bond cleavage involved in this catalytic decarbonylation reaction of tropone derivatives.

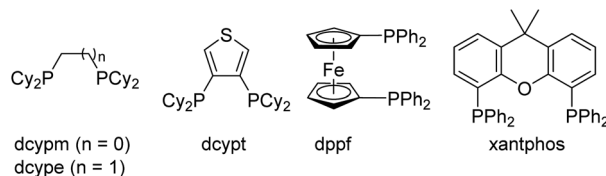
To examine the catalyst turnover process, we next investigated the catalytic activity of  $\text{Ni(CO)}_3(\text{IMes}^{\text{Me}})$ , which would be expected to be formed as the decarbonylation reaction proceeds (Scheme 1a). It was found that  $\text{Ni(CO)}_3(\text{IMes}^{\text{Me}})$  successfully catalyzed the decarbonylation of tropone **1e** (94% yield). This result is in sharp contrast to the fact that this carbonyl complex does not catalyze the decarbonylation of simple ketones, which is the major reason for unsuccessful catalytic reactions.<sup>9a</sup> Therefore, the C(acyl)–C bond in **1e** is more reactive than a corresponding bond of simple ketones because of vdW strain and can be activated by a less reactive CO-bound nickel species, allowing for a catalyst turnover. Indeed, the decarbonylation of **1e** proceeded even at ambient temperature in 61% yield when a stoichiometric amount of a nickel complex was used (Scheme 1b), suggesting that a high temperature of 160 °C is required to release a CO ligand to regenerate an active Ni(0) species.

### Catalytic two-carbon ring contraction reactions

During our optimization study of the decarbonylation of **1e**, we envisioned that the use of a bidentate ligand would help to release a CO ligand from Ni(0) species, thereby improving the catalyst turnover step.<sup>9b,c</sup> Although these trials did not give satisfactory results for this decarbonylation, we noticed that a cyclopentadiene **3e** was also formed in 8% yield, which appeared to be produced *via* the formal loss of CO and PhC units, when dcype was used as the ligand (Table 2, entry 1; Table S1, entry 6 in the ESI† for details), whereas no **3e** was observed when NHCs or monodentate phosphine ligands, such as  $\text{PCy}_3$ , were used (Table S1,† entries 1–5 and 7). The unexpected formation of **3e** led us to re-examine the reaction conditions

Table 2 Nickel-catalyzed two-carbon ring contraction of tropone **1e**<sup>a</sup>

Entry	Ligand	Additive	Isolated yields (%)		
			3e	2e	Recovered 1e
1 <sup>b</sup>	dcype	None	8	20	67
2	dcype	None	6	8	59
3	dcypm	None	11	18	55
4	dcypt	None	9	7	65
5	Dppf	None	15	9	76
6	Xantphos	None	12	2	84
7	dcype	MeOH	>99	0	0
8	dcype	EtOH	53	0	21
9	dcype	2-Propanol	24	0	10

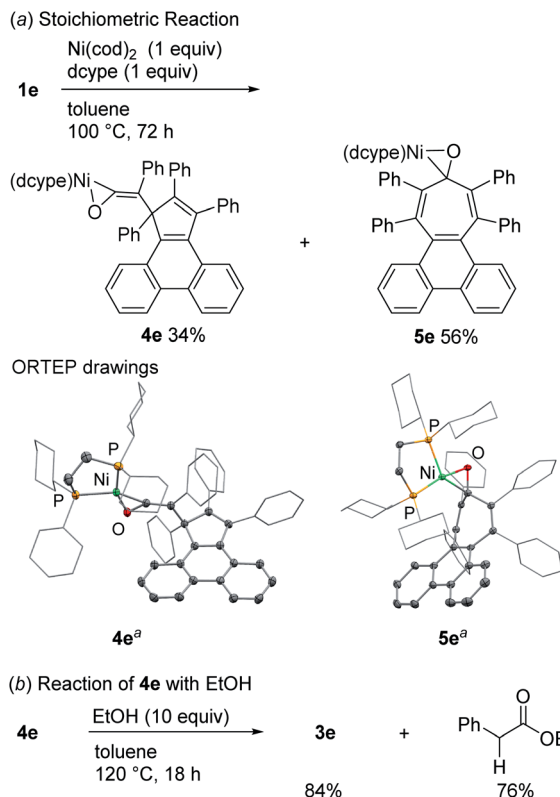


<sup>a</sup> Reaction condition: **1e** (0.1 mmol),  $\text{Ni(cod)}_2$  (0.020 mmol), ligand (0.020 mmol),  $\text{NaO}^t\text{Bu}$  (0.020 mmol), toluene (1.0 mL), 120 °C for 18 h. <sup>b</sup> Run at 160 °C. NMR yields.

with respect to the selective formation of **3e** (Table 2). The generation of the decarbonylated product **2e** was suppressed when the reaction was performed at 120 °C (entry 2). A brief screening of ligands and additives revealed that the use of other bidentate phosphines also gave the desired two-carbon elimination product **3e**, although the highest yield was only 15% (entries 3–6). Considering that a hydrogen atom is incorporated during the formation of **3e**, we subsequently examined the addition of a hydrogen source to the reaction mixture (entries 7–9). As a result, **3e** was selectively formed quantitatively, when the nickel/dcype-catalyzed reaction of **1e** was carried out in the presence of MeOH (10 equiv.) (entry 7). Importantly, under these conditions,  $\text{PhCH}_2\text{CO}_2\text{Me}$  was also formed (80% yield), suggesting that the rest of the fragment of **1e** was eliminated as 2-phenylethen-1-one (phenylketene), which was trapped by the added MeOH. To the best of our knowledge, this reaction represents the first catalytic conversion of a tropone ring system into a five-membered ring skeleton.

To obtain insights into the mechanism responsible for the generation of **3e**, a stoichiometric reaction of **1e**,  $\text{Ni(cod)}_2$  and dcype was performed in toluene at 100 °C, which led us to isolate the nickel–ketene complex **4e**<sup>19,20</sup> in 34% yield, along with **5e** (56%) (Scheme 2a). The isolated ketene complex **4e** was converted into the cyclopentadiene **3e** in 84% yield by heating in toluene at 120 °C in the presence of EtOH (10 equiv.) (Scheme

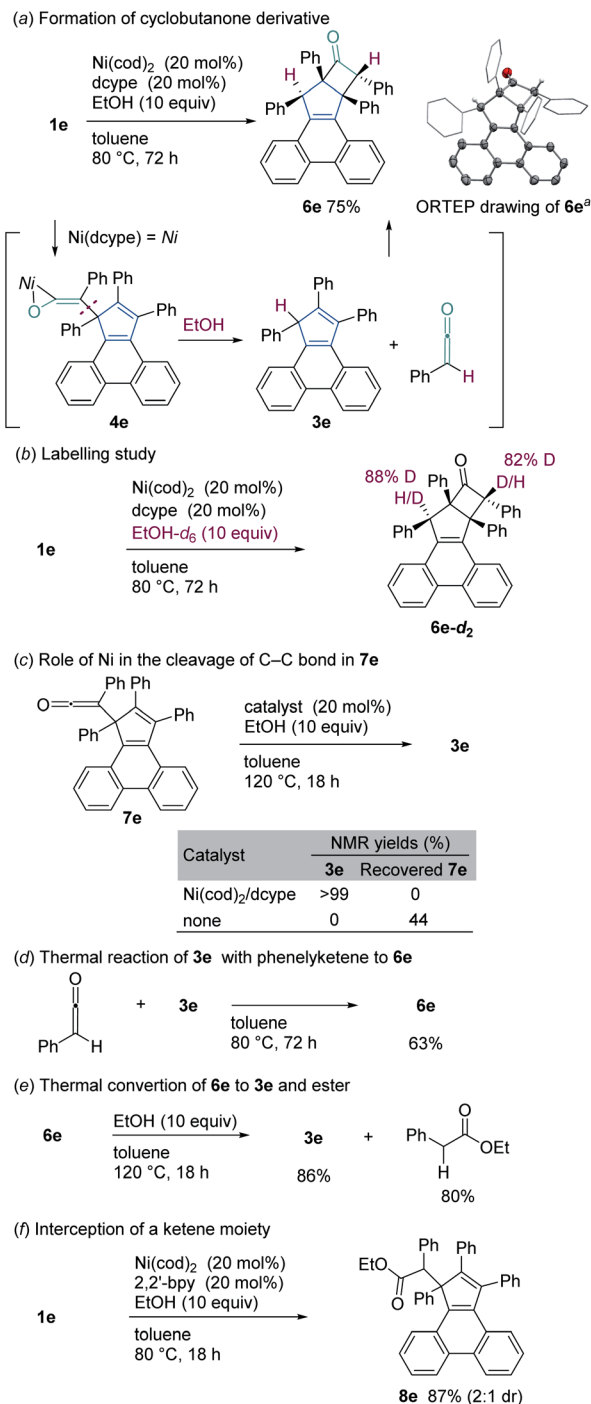




Scheme 2 Intermediacy of a nickel–ketene complex. <sup>a</sup>ORTEP drawings depicted at the 50% probability level. Hydrogen atoms were omitted for clarity. Phenyl and cyclohexyl groups were depicted as wireframe model.

2b). In this reaction,  $\text{PhCH}_2\text{CO}_2\text{Et}$  was also formed in 76% yield, indicating that the ketene fragment in  $\mathbf{4e}$  is reductively cleaved<sup>21</sup> to give the cyclopentadiene  $\mathbf{3e}$  and a phenylketene, the latter of which was trapped by EtOH to form  $\text{PhCH}_2\text{CO}_2\text{Et}$ .

To collect additional mechanistic details for the conversion of the ketene complex  $\mathbf{4e}$  to cyclopentadiene  $\mathbf{3e}$ , we examined the Ni/dcpye-catalyzed reaction of  $\mathbf{1e}$  with EtOH at lower temperature (Scheme 3a). As a result, when the reaction was carried out at 80 °C, the cyclobutanone derivative  $\mathbf{6e}$  was formed in 75% yield. This transformation is not a simple skeletal isomerization, but two additional hydrogen atoms were incorporated into  $\mathbf{1e}$ . The generation of  $\mathbf{6e}$  could be explained as follows. The C–C bond that connects a cyclopentadiene scaffold and a ketene moiety in complex  $\mathbf{4e}$  is reductively cleaved<sup>4a,21,22</sup> in the presence of EtOH to afford phenylketene ( $\text{PhCH}=\text{C}=\text{O}$ ) and  $\mathbf{3e}$ , which subsequently undergoes a formal hetero [2 + 2] cycloaddition with the formation of the cyclobutanone  $\mathbf{6e}$  (Scheme 3a). Labelling experiments using EtOH-*d*<sub>6</sub> confirmed that the two hydrogen atoms that are incorporated into  $\mathbf{6e}$  are derived from EtOH (Scheme 3b). An independently synthesized nickel-free ketene  $\mathbf{7e}$  could be converted to  $\mathbf{3e}$  in a quantitative yield when a Ni/dcpye catalyst was used (Scheme 3c). In contrast,  $\mathbf{6e}$  did not undergo C–C bond fission under thermal conditions, but rather the addition of EtOH to a ketene moiety occurred to form  $\mathbf{8e}$  in 33% yield (see Scheme 3f for the

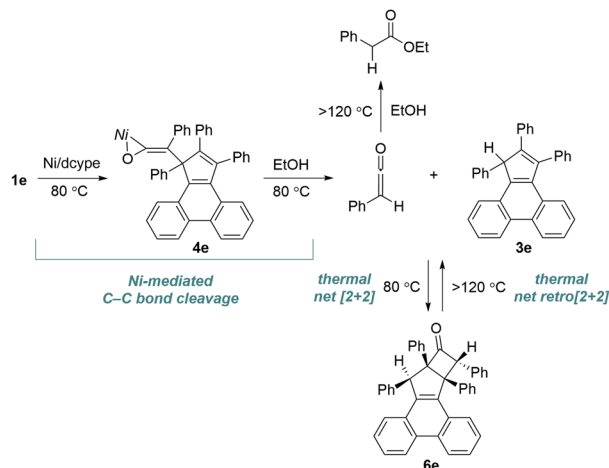


Scheme 3 Additional mechanistic studies. <sup>a</sup>ORTEP drawing of  $\mathbf{6e}$  depicted at the 50% probability level. Hydrogen atoms were omitted for clarity. Phenyl and cyclohexyl groups were depicted as wireframe model 2,2'-bpy = 2,2'-bipyridine.

structure of  $\mathbf{8e}$ ), suggesting that the nickel catalyst plays an active role in the C–C bond cleavage step. The reaction between  $\text{PhCH}=\text{C}=\text{O}$  and  $\mathbf{3e}$  proceeded thermally (in toluene at 80 °C for 72 h) to afford  $\mathbf{6e}$  in 63% yield (Scheme 3d). It is noteworthy that a thermal reaction between ketene and cyclopentadiene was reported to form cyclobutanone derivatives *via* a [4 + 2]







Scheme 4 Pathways involved in the conversion of tropone **1e** to cyclopentadiene **3e**.

cycloaddition/[3,3]-sigmatropic rearrangement sequence, resulting in a net [2 + 2] cycloaddition.<sup>20</sup> Cyclobutanone **6e** could be converted into **3e** in 84% yield *via* a thermally-induced formal *retro*-[2 + 2] cycloaddition reaction at 120 °C (Scheme 3e). Additional studies revealed that the use of 2,2'-bipyridine allows for the addition of EtOH to the ketene moiety of **7e**, providing a new cyclopentadiene derivative **8e** (Scheme 3f). This result further highlights the profound impact of the ligand on the course of these types of reactions.

On the basis of the mechanistic findings shown in Schemes 2 and 3, the nickel/dcype-mediated reaction of **1e** can be summarized as depicted in Scheme 4. The isomerization of tropone **1e** to the ketene complex **4e** initially occurs at 80 °C. Subsequent nickel-mediated C–C bond cleavage occurs at 80 °C in the presence of EtOH with the formation of the cyclopentadiene **3e** and phenylketene, which then undergo

a thermally-induced formal [2 + 2] cycloaddition to form cyclobutanone **6e**. At higher temperatures, the reverse process from **6e** to **3e** begins to occur, leading to these compounds being in equilibrium. The phenylketene slowly and irreversibly reacts with EtOH at 120 °C (ref. 23) to form an ester (PhCH<sub>2</sub>CO<sub>2</sub>Et), thereby allowing for a selective formation of **3e** at this temperature. Indeed, density functional theory (DFT) calculations at the M06-2X/6-31G(d,p) level of theory suggested that the sum of Gibbs free energies of **3e** and PhCH<sub>2</sub>CO<sub>2</sub>Et is thermodynamically more stable than the sum of those for **6e** and EtOH ( $\Delta G = -25.9$  kcal mol<sup>-1</sup>).

### Computational studies

Reaction mechanisms and ligand-controlled selectivity for both types of ring contraction reactions were also investigated by DFT calculations at the M06-2X/6-31G(d,p)-LanL2DZ level of theory (see ESI† in details). The mechanism for the oxidative addition of a C–C bond was initially investigated when IMes<sup>Me</sup> was used as a ligand. The coordination of **1e** to Ni(IMes<sup>Me</sup>) forms **Int I**, in which the C1'–C2' bond of a phenyl group at the  $\alpha$ -position coordinates in a  $\eta^2$  manner, which is followed by the oxidative addition of a C1–C2 bond proceed *via* three-centred transition state **TS I** to give **Int II**. The activation barrier for this process is lower for **1e** (11.7 kcal mol<sup>-1</sup>) than that for unreactive substrates such as **1c** (28.2 kcal mol<sup>-1</sup>) and **1h** (21.6 kcal mol<sup>-1</sup>) (Fig. 2a). The results of a distortion/interaction analysis<sup>24</sup> indicated that the distortion energy ( $\Delta E_{\text{strain}}^\ddagger$ ) of Ni–IMes<sup>Me</sup> and **1e** for **TS I** is smaller compared with that for **1c** or **1h** (see Table S2 in ESI†). In contrast, the difference in the interaction energy ( $\Delta E_{\text{int}}^\ddagger$ ) for these fragments for **TS I** is relatively small. The smaller  $\Delta E_{\text{strain}}^\ddagger$  of Ni–IMes<sup>Me</sup> and **1e** indicates that **1e** possesses a larger strain that originates from vdW repulsion between the bulky substituents compared to **1c** or **1h**, thereby leading to a lower activation barrier for this oxidative addition process. In contrast, when bidentate dcype is used as the ligand,

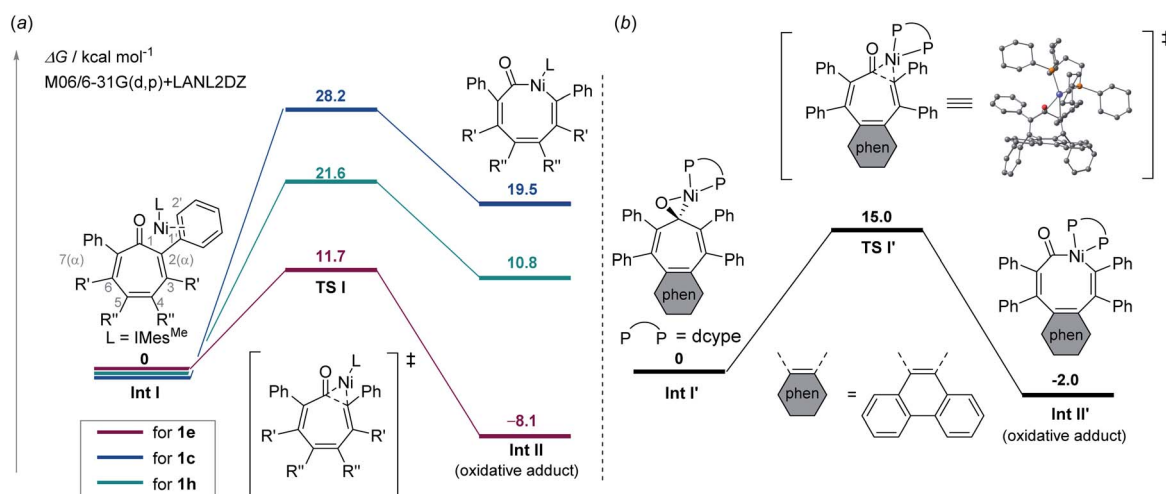


Fig. 2 (a) Substrate dependence on the oxidative addition of **1e** (red), **1c** (blue), and **1h** (green) to Ni–IMes<sup>Me</sup>. For **1h**, an  $\alpha$ -phenyl analogue was used as a model for clarity. (b) Oxidative addition of **1e** to Ni–dcype at the at the M06-2X/6-31G(d,p)-LanL2DZ level of theory.



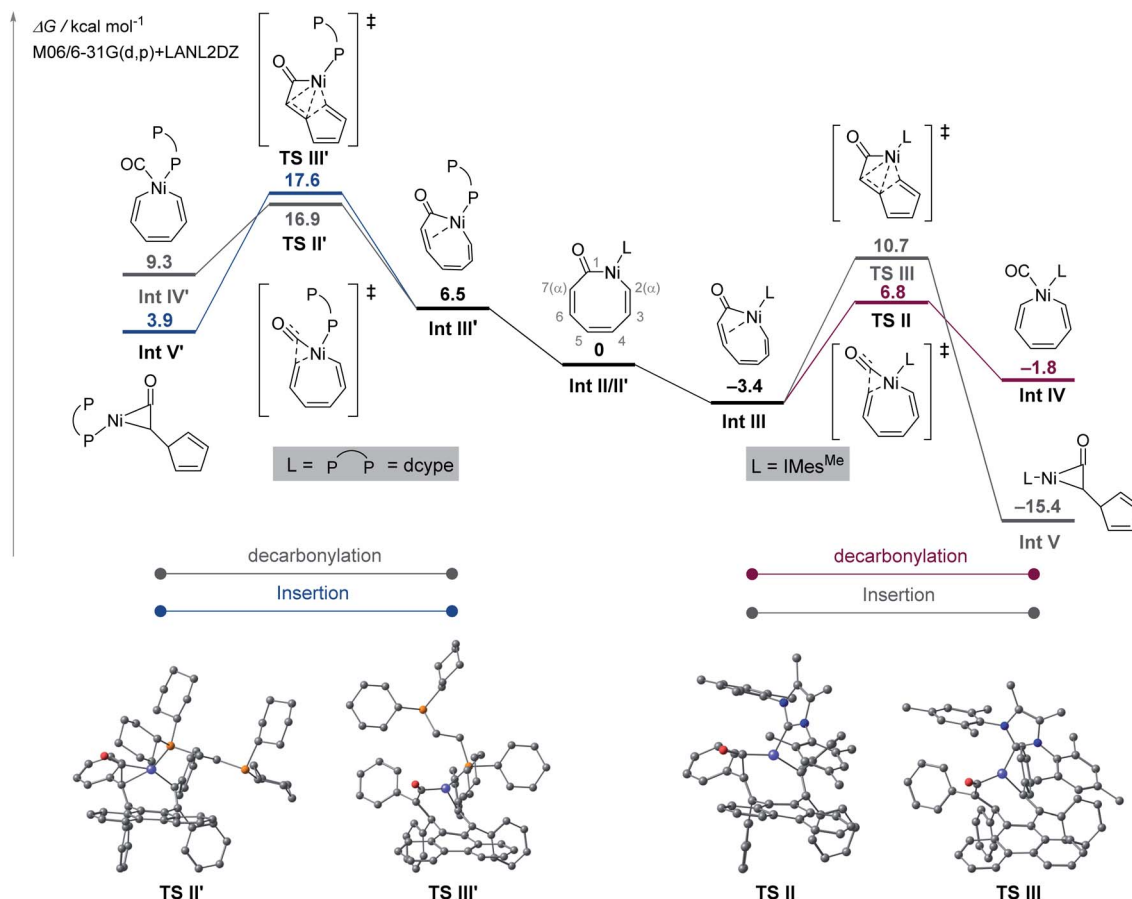
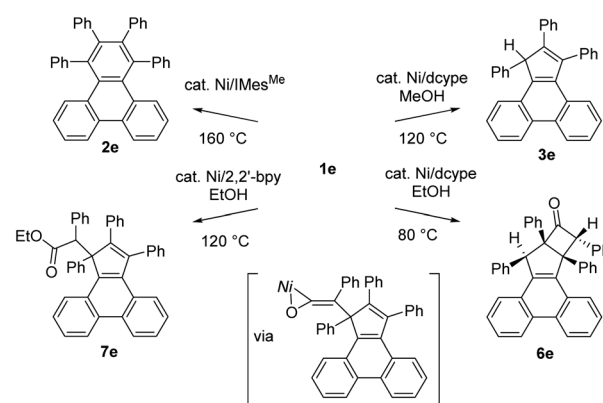


Fig. 3 Energy diagram for ligand-controlled selective ring contraction reactions of **1e** at the M06-2X/6-31G(d,p)-LanL2DZ level of the theory.

oxidative addition occurs from the  $\eta^2$ -(C=O) coordinated Ni(0)-dcype intermediate (*i.e.*, **Int I'**) via three-centred transition state **TS I'** to generate **Int II'**. The activation barrier for this oxidative addition is higher than that for Ni-IMes<sup>Me</sup> (15.0 kcal mol<sup>-1</sup>) (Fig. 2b). The calculated activation barriers for oxidative addition of **1e** are low for both IMes<sup>Me</sup> and dcype ligands, suggesting that the initial oxidative addition is not the rate-determining step of the decarbonylation reaction and high temperature is required for the dissociation of CO from Ni(0).

The ligand-controlled selectivity was next examined by exploring the reaction pathways after the oxidative addition complexes **Int II/Int II'** had been formed (Fig. 3). Using IMes<sup>Me</sup> as the ligand, **Int II** undergoes decarbonylation via **Int III**, in which the C6–C7 double bond of the nickelacycle coordinates to the nickel centre, with a reasonable activation barrier of 10.2 kcal mol<sup>-1</sup>. The activation barrier for the competitive intramolecular insertion (ketene formation) process<sup>25</sup> is higher by 3.9 kcal mol<sup>-1</sup> compared to that for decarbonylation, thus rendering the decarbonylation pathway kinetically more favoured. When dcype is used as the ligand, **Int II'** is converted to **Int III'** by the coordination of an intramolecular alkene with one of the phosphorus atoms of dcype being dissociated. Although

the difference in the activation barriers for the subsequent decarbonylation (*i.e.*, the formation of **Int IV'**) and ketene formation (*i.e.*, the formation of **Int V'**)<sup>25</sup> steps is less than 1 kcal mol<sup>-1</sup>, the formation of **Int V'** is exergonic, which explains the selective formation of cyclopentadiene in the case of a dcype ligand (Fig. 3).



Scheme 5 Catalyst controlled-conversion of **1e** to diverse ring systems.



## Conclusions

In conclusion, we report on C–C bond cleavage reactions of tropone derivatives by nickel catalysis. When NHC is used as a ligand, the decarbonylation reaction proceeds catalytically to form a benzene ring (one-carbon ring contraction). In contrast, when dcype is used as the ligand, the tropone derivatives undergo a two-carbon ring contraction with the formation of cyclopentadiene derivatives. The addition of alcohol is essential for an efficient reaction, and the dissociated ketene fragment can be trapped by the cyclopentadiene moiety to generate polycyclic cyclobutanone derivatives. X-ray crystallography studies revealed that the formation of these compounds involves a nickel-ketene intermediate, which can be trapped by EtOH catalytically by changing the ligand from dcype to 2,2'-bipyridine. The judicious selection of the ligand and reaction temperature enables four different products, including three different ring systems, to be produced catalytically from a single substrate (Scheme 5).

## Data availability

All experimental and characterization data are available in the ESI.† Crystallographic data for compounds **c1**, **1i**, **4e**, **5e**, **6e**, **8e**, and Ni(CO)<sub>3</sub>(IMes<sup>Me</sup>) have been deposited in the Cambridge Crystallographic Data Centre under accession numbers CCDC 2115589–2115595.

## Author contributions

T. K. and M. T. conceived the project. T. K. and K. S. performed the experimental work. T. K. and K. S. collected and analysed the spectroscopic data. T. K. and M. T. wrote the manuscript. All of the authors discussed the results and contributed to the preparation of the manuscript.

## Conflicts of interest

There are no conflicts to declare.

## Acknowledgements

This work was supported by Grant-in-Aid for Early-Career Scientists (JP19K15564), Grant-in-Aid for Scientific Research (A) (JP21H04682) from MEXT, Japan and TOBE MAKI Scholarship Foundation (20-JA-013). We thank the Instrumental Analysis Center, Faculty of Engineering, Osaka University, for their assistance with HRMS.

## Notes and references

- Selected reviews: (a) M. Murakami, *Cleavage of Carbon–Carbon Single Bonds by Transition Metals*, in *Activation of Unreactive Bonds and Organic Synthesis*, Springer-Verlag Berlin Heidelberg, 1999, pp. 97–129; (b) F. Chen, T. Wang and N. Jiao, *Chem. Rev.*, 2014, **114**, 8613–8661; (c) *C–C Bond Activation*, ed. G. Dong, Springer-Verlag Berlin Heidelberg, 2014; (d) *Cleavage of Carbon-Carbon Single Bonds by Transition Metals*, ed. M. Murakami and N. Chatani, Wiley-VCH Verlag GmbH & Co. KGaA, 2015; (e) L. Souillart and N. Cramer, *Chem. Rev.*, 2015, **115**, 9410–9464; (f) M. Murakami and N. Ishida, *J. Am. Chem. Soc.*, 2016, **138**, 13759–13769; (g) P.-H. Chen, B. A. Billett, T. Tsukamoto and G. Dong, *ACS Catal.*, 2017, **7**, 1340–1360; (h) Z. Nairoukh, M. Cormier and I. Marek, *Nat. Rev. Chem.*, 2017, **1**, 0035; (i) F. Song, T. Gou, B.-Q. Wang and Z.-J. Shi, *Chem. Soc. Rev.*, 2018, **47**, 7078–7115; (j) L. Deng and G. Dong, *Trends Chem.*, 2020, **2**, 183–198; (k) H. Lu, T.-Y. Yu, P. F. Xu and H. Wei, *Chem. Rev.*, 2021, **121**, 365–411.
- Selected reviews: (a) M. Rubin, M. Rubina and V. Gevorgyan, *Chem. Rev.*, 2007, **107**, 3117–3179; (b) L. Jiao and Z.-X. Yu, *J. Org. Chem.*, 2013, **78**, 6842–6848; (c) T. Seiser, T. Saget, D. N. Tran and N. Cramer, *Angew. Chem., Int. Ed.*, 2011, **50**, 7740–7752; (d) P.-H. Chen and G. Dong, *Chem.–Eur. J.*, 2016, **22**, 18290–18315; (e) D. J. Mack and J. T. Njardarson, *ACS Catal.*, 2013, **3**, 272–286; (f) G. Fumagalli, S. Stanton and J. F. Bower, *Chem. Rev.*, 2017, **117**, 9404–9432; (g) R. Vicente, *Chem. Rev.*, 2021, **121**, 162–226.
- Selected reviews: (a) Y. J. Park, J.-W. Park and C.-H. Jun, *Acc. Chem. Res.*, 2008, **41**, 222–234; (b) D.-S. Kim, W.-J. Park and C.-H. Jun, *Chem. Rev.*, 2017, **117**, 8977–9015; (c) Y. Xia and G. Dong, *Nat. Rev. Chem.*, 2020, **4**, 600–614; Selected examples:; (d) M. Gozln, A. Weisman, Y. Ben-David and D. Milstein, *Nature*, 1993, **364**, 699–701; (e) J. Zhu, J. Wang and G. Dong, *Nat. Chem.*, 2019, **11**, 45–51; (f) S. Sakurai and M. Tobisu, *Organometallics*, 2019, **38**, 2834–2838; (g) J. Zhu, R. Zhang and G. Dong, *Nat. Chem.*, 2021, **13**, 836–842.
- (a) R. B. King and A. Efraty, *J. Am. Chem. Soc.*, 1972, **94**, 3773–3779; (b) R. H. Crabtree, R. P. Dion, D. J. Gibboni, D. V. Mcgrath and E. M. Holt, *J. Am. Chem. Soc.*, 1986, **108**, 7222–7227; (c) M. A. Halcrow, F. Urbanos and B. Chaudret, *Organometallics*, 1993, **12**, 955–957; (d) S. W. Youn, B. S. Kim and A. R. Jagdale, *J. Am. Chem. Soc.*, 2012, **134**, 11308–11311; (e) G. Smits, B. Audic, M. D. Wodrich, C. Corminboeuf and N. Cramer, *Chem. Sci.*, 2017, **8**, 7174–7179; (f) Y. Xu, X. Qi, P. Zheng, C. C. Berti, P. Liu and G. Dong, *Nature*, 2019, **567**, 373–378; Review: ; (g) F. Hu, L. Wang, L. Xu and S.-S. Li, *Org. Chem. Front.*, 2020, **7**, 1570–1575.
- Selected reviews: (a) M. D. R. Lutz and B. Morandi, *Chem. Rev.*, 2021, **121**, 300–326; (b) K. Nogi and H. Yorimitsu, *Chem. Rev.*, 2021, **121**, 345–364.
- Selected reviews: (a) M. Tobisu and N. Chatani, *Chem. Soc. Rev.*, 2008, **37**, 300–307; (b) M. Tobisu, *Reactions via Cleavage of Carbon–Carbon Bonds of Ketones and Nitriles*, in *Cleavage of Carbon-Carbon Single Bonds by Transition Metals*, Wiley-VCH Verlag GmbH & Co. KGaA, 2015, pp. 193–220; (c) Y. Nakao, *Chem. Rev.*, 2021, **121**, 327–344.
- M. Murakami, H. Amii and Y. Ito, *Nature*, 1994, **370**, 540–541.
- O. Daugulis and M. Brookhart, *Organometallics*, 2004, **23**, 527–534.
- (a) T. Morioka, A. Nishizawa, T. Furukawa, M. Tobisu and N. Chatani, *J. Am. Chem. Soc.*, 2017, **139**, 1416–1419; Our group also reported on nickel-catalyzed decarbonylation of



- amides and acylsilanes via C–C bond cleavage;; (b) T. Morioka, S. Nakatani, Y. Sakamoto, T. Kodama, S. Ogoshi, N. Chatani and M. Tobisu, *Chem. Sci.*, 2019, **10**, 6666–6671; (c) S. Nakatani, Y. Ito, S. Sakurai, T. Kodama and M. Tobisu, *J. Org. Chem.*, 2020, **85**, 7588–7594.
- 10 K. Kaneda, H. Azuma, M. Wayaku and S. Tehanishi, *Chem. Lett.*, 1974, **3**, 215–216.
- 11 (a) J. Blum, E. Oppenheimer and E. D. Bergmann, *J. Am. Chem. Soc.*, 1967, **89**, 2338–2341; (b) S. Murahashi, T. Naota and N. Nakajima, *J. Org. Chem.*, 1986, **51**, 898–901; (c) K. Nozaki, N. Sato and H. Takaya, *J. Org. Chem.*, 1994, **59**, 2679–2681; (d) Y. Nishihara, Y. Inoue, M. Itazaki and K. Takagi, *Org. Lett.*, 2005, **7**, 2639–2641; (e) Y. Kobayashi, H. Kamisaki, R. Yanada and Y. Takemoto, *Org. Lett.*, 2006, **8**, 2711–2713; (f) Y. Nakao, Y. Hirata and T. Hiyama, *J. Am. Chem. Soc.*, 2006, **128**, 7420–7421.
- 12 (a) A. Dermenci, R. E. Whittaker and G. Dong, *Org. Lett.*, 2013, **15**, 2242–2245; (b) A. Dermenci, R. E. Whittaker, Y. Gao, F. A. Cruz, Z.-X. Yu and G. Dong, *Chem. Sci.*, 2015, **6**, 3201–3210.
- 13 Selected examples: (a) N. Chatani, Y. Ie, F. Kakiuchi and S. Murai, *J. Am. Chem. Soc.*, 1999, **121**, 8645–8646; (b) Z.-Q. Lei, H. Li, Y. Li, X.-S. Zhang, K. Chen, X. Wang, J. Sun and Z.-J. Shi, *Angew. Chem., Int. Ed.*, 2012, **51**, 2690–2694; (c) R. Zeng and G. Dong, *J. Am. Chem. Soc.*, 2015, **137**, 1408–1411; (d) R. Zeng, P. H. Chen and G. Dong, *ACS Catal.*, 2016, **6**, 969–973; (e) Z.-Q. Lei, F. Pan, H. Li, Y. Li, X.-S. Zhang, K. Chen, X. Wang, Y.-X. Li, J. Sun and Z.-J. Shi, *J. Am. Chem. Soc.*, 2015, **137**, 5012–5020; (f) C. Jiang, W.-Q. Wu, H. Lu, T.-Y. Yu, W.-H. Xu and H. Wei, *Asian J. Org. Chem.*, 2019, **8**, 1358–1362; (g) C. Jiang, Z.-J. Zheng, T.-Y. Yu and H. Wei, *Org. Biomol. Chem.*, 2018, **16**, 7174–7177; (h) T.-T. Zhao, W.-H. Xu, Z.-J. Zheng, P.-F. Xu and H. Wei, *J. Am. Chem. Soc.*, 2018, **140**, 586–589; (i) T.-Y. Yu, W.-H. Xu, H. Lu and H. Wei, *Chem. Sci.*, 2020, **11**, 12336–12340.
- 14 Selected examples: (a) C.-H. Jun and H. Lee, *J. Am. Chem. Soc.*, 1999, **121**, 880–881; (b) Y. Xia, G. Lu, P. Liu and G. Dong, *Nature*, 2016, **539**, 546–550; (c) J. Zhong, W. Zhou, X. Yan, Y. Xia, H. Xiang and X. Zhou, *Org. Lett.*, 2022, **24**, 1372–1377.
- 15 Selected reviews on tropones, see: (a) P. L. Pauson, *Chem. Rev.*, 1955, **55**, 9–136; (b) F. Pietra, *Chem. Rev.*, 1973, **73**, 293–364; (c) F. Pietra, *Acc. Chem. Res.*, 1979, **12**, 132–138.
- 16 (a) T. Murai, T. Nakazawa and T. Shishido, *Tetrahedron Lett.*, 1967, **8**, 2465–2469; (b) T. Murai and T. Sato, *Bull. Chem. Soc. Jpn.*, 1968, **41**, 2819.
- 17 (a) T. Kodama, Y. Kawashima, Z. Deng and M. Tobisu, *Inorg. Chem.*, 2021, **60**, 4332–4336; (b) T. Kodama, Y. Kawashima, K. Uchida, Z. Deng and M. Tobisu, *J. Org. Chem.*, 2021, **86**, 13800–13807; A similar X-ray crystal structure of **1c** was reported; see: (c) K. Ibata, H. Shimanouchi and Y. Sasada, *Acta Cryst.*, 1977, **B33**, 1129–1138.
- 18 A similar ground state destabilization by vdW strain is frequently utilized in the C–N bond activation of amides. A leading review: G. Meng, J. Zhang and M. Szostak, *Chem. Rev.*, 2021, **121**, 12746–12783.
- 19 (a) The structure of **4e** was unambiguously determined by X-ray crystallography (Fig. S8 in ESI†); (b) Related Ni/ketene complexes: N. D. Staudaher, A. M. Arif and J. Louie, *J. Am. Chem. Soc.*, 2016, **138**, 14083–14091.
- 20 (a) S. Yamabe, T. Dai, T. Minato, T. Machiguchi and T. Hasegawa, *J. Am. Chem. Soc.*, 1996, **118**, 6518–6519; (b) T. Machiguchi, T. Hasegawa, A. Ishiwata, S. Terashima, S. Yamabe and T. Minato, *J. Am. Chem. Soc.*, 1999, **121**, 4771–4786.
- 21 Although the detailed mechanism responsible for this process is unclear, C–C bond cleavage is likely to be driven by aromatization (*i.e.*, formation of cyclopentadienyl anion). See ref. 4a for a related reaction in this context.
- 22 The overall process is a reductive C–C bond cleavage, in which two hydrogen atoms are incorporated. The results of labelling studies confirmed that an external alcohol serves as the hydride source (Scheme 3b).  $\beta$ -Hydrogen elimination of metal–alkoxide species is presumably involved. For example, see: K. Yasui, M. Higashino, N. Chatani and M. Tobisu, *Synlett*, 2017, **28**, 2569–2572.
- 23 The thermal reaction of PhCH=C=O with EtOH in toluene was slower (19% at 80 °C; 59% at 120 °C for 72 h) than that with the cyclopentadiene **3e** (see ESI†), which is also consistent with the mechanistic scheme shown in Scheme 4.
- 24 F. M. Bickelhaupt and K. N. Houk, *Angew. Chem., Int. Ed.*, 2017, **56**, 10070–10086.
- 25 The isomerization to a cyclopentadiene derivative is a concerted process that proceeds via **TSIII/III'** in which C2 and C6 carbons are located close to facilitate the bond formation between these carbons.

